Journal of Applied Sciences

ISSN 1812-5654

science alert

ANSInet
an open access publisher
http://ansinet.com

Journal of Applied Sciences 11 (17): 3070-3088, 2011
ISSN 1812-5654 / DOI: 10.3923/jas.2011.3070.3088

Provenance and Source Area Weathering Derived from the Geochemistry of Pre-Cenomanian Sandstones, East Sinai, Egypt

Adel I.M. Akarish and Amr M. El-Gohary
Department of Geological Sciences, National Research Centre, El Tahrir Street,
Dokki, Cairo, Egypt

Abstract: The study aimed at characterizing the geochemical compositions of the pre-Cenomanian sandstones of Gebel Ghazalani area, east Sinai. X-Ray Fluorescence (XRF), Induced Coupled Plasma-Mass Spectrometry (ICP-MS) and Induced Coupled Plasma-Emission Spectrometry (ICP-ES) analyses were used to determine the sandstone composition. Major, trace and rare earth element compositions of the sandstones have been investigated to determine their provenance, tectonic setting and the influence of weathering conditions. The studied succession (~214 m thick) starts by undifferentiated pre- Carboniferous sediments that unconformably overlies the Katherina Volcanics and followed upwards by the Lower Cretaceous sandstones of the Malha Formation. The pre-Cenomanian sandstones are enriched in SiO_2 and High Field Strength Elements (HFSE) and are depleted in mobile elements, Large-Ion Lithophile Elements (LILE), transition metals and possess low contents of TiO_2 and Fe_2O_3. Their Rare Earth Elements (REE) pattern displays high Light REE/Heavy REE (LREE/ HREE) ratio, flat HREE and a significant negative Eu anomaly. The source area may have contained quartzose sedimentary rocks. The geochemical data support deposition in a passive continental margin and the sediments were derived from felsic (granitic) source rocks. Trace and REE data as well as the high values of the weathering indices: Chemical Index of Alteration (CIA), Plagioclase Index of Alteration (PIA) and Chemical Index of Weathering (CIW) suggest moderate to extreme weathering conditions in the source area or during transportation. Also, they indicate that recycling processes might have been significant. Clay content, zircons and quartz dilution are responsible for the variation in REE contents.

Key words: Geochemistry, source rocks, tectonic setting, paleo-weathering, siliciclastics, Sinai

INTRODUCTION

The use of geochemical composition of siliciclastic sedimentary rocks is an vital tool to know the nature of source rocks (Roser and Korsch, 1988; McLennan *et al*., 1993; Ajayi *et al*., 2006), weathering and erosion dynamics (Nesbitt and Young, 1982), the tectonic setting of the depositional basins (Bhatia, 1983; Bhatia and Crook, 1986; Roser and Korsch, 1986) and post-depositional changes (Fedo *et al*., 1995, 1996). Utilizing geochemical data from sediments to understand such sedimentary processes are growing in the literature due to the sensitiveness of some key trace elements in identifying minor components that are not easily recognized petrographically (Garver *et al*., 1996; Gallala *et al*., 2009; Abd El-Rahman *et al*., 2010).

The pre-Cenomanian sedimentary rocks are exposed at many localities in East Sinai. They are formed of Nubian type sandstones that are related to the Early Paleozoic-Early Cretaceous age. They overlie unconformably the Precambrian Basement complex and underlie the marine Cenomanian shales and marls. Continental to shallow marine facies have been recognized (El-Kelany and Said, 1990; Issawi *et al*., 1999). Rather localized studies related to the sandstones of Nubia Facies exposures of East Sinai were carried out by some workers (El-Kelany and Said, 1990; Kora, 1991; Akarish, 1998; Issawi *et al*., 1999; Salem *et al*., 2001; Akarish and El-Gohary, 2008). Most of these studies deal with their stratigraphy, sedimentology and petrology.

The pre-Cenomanian sandstones composition, provenance and tectonic setting of G. Ghazalani area have not yet been examined. Moreover, there is no work on the geology of this area, may be due to the difficulty of access. In this study, mineralogical and geochemical data of rocks constituting the selected sequence in the eastern portion of Sinai are reported. The main aim of this study is to investigate the provenance and tectonic setting and attempt to shed light on source area paleo-weathering conditions.

Corresponding Author: Adel I.M. Akarish, Department of Geological Sciences, National Research Centre, El Tahrir Street, Dokki, Cairo, Egypt Tel: 002-010-1136468

GEOLOGIC SETTING AND LITHOSTRATIGRAPHY

Gebel Ghazalani area is located in the northeastern part of Sinai, near the northwestern end of the Gulf of Aqaba (Fig. 1). In the studied area and the areas adjacent to the Gulf of Aqaba, the pre-rifting rocks consist mainly of Precambrian plutonic and metamorphic rocks and a sedimentary cover, which includes pre-Cenomanian Nubian type sandstones (Early Paleozoic-Early Cretaceous) followed upwards by Cenomanian to Eocene strata dominated by carbonate rocks. According to Abd El-Khalek *et al.* (1993), the rifting process resulted in wrenching deformation which represented by major strike-slip faults and associated folds. These faults are of NNE sinistral slip and N-W ones that are of dextral slip and cutting through the pre-rift Basement complex and the overlying sedimentary rocks. In the study area, the oldest exposed rocks are represented by alkaline rocks related to the Katherina Volcanics (Samuel *et al*., 2007). These volcanics are unconformably overlain by Early Paleozoic-Lower Cretaceous sandstones followed by the marine Cenomanian shales and marls (Raha Formation) and terminated by Turonian sequence formed of shales and limestones (Abu Qada and Wata Formations).

Kostandi (1959) and Said (1962) ascribed the Early Paleozoic sandstone of East Sinai as pre-Carboniferous and may include Cambrian rocks as indicated by Said, (1971). On the other hand, El-Kelany and Said (1990) divided the Early Paleozoic rocks in East Sinai, from base to top into: Taba, Araba and Naqus Formations. They advocated without strong proofs that these formations belong to the Infracambrian, Cambrian and Cambrian-Ordovician, respectively.

The pre-Cenomanian succession (Early Paleozoic-Early Cretaceous) in Gebel Ghazalani area is about 214 m thick composed of continental siliciclastic sediments (Fig. 2). These sediments are varicolored, unfossiliferous, cross-bedded medium-to fine-grained sandstones with thin clay rich interbeds (marlstone/argillaceous sandstone). In general, the studied sequences is characterized by trough cross-bedding, ripple cross-lamination with fining upwards and complete absence of evaporates and calcareous rocks support deposition under fluvial conditions. Within this sandstone

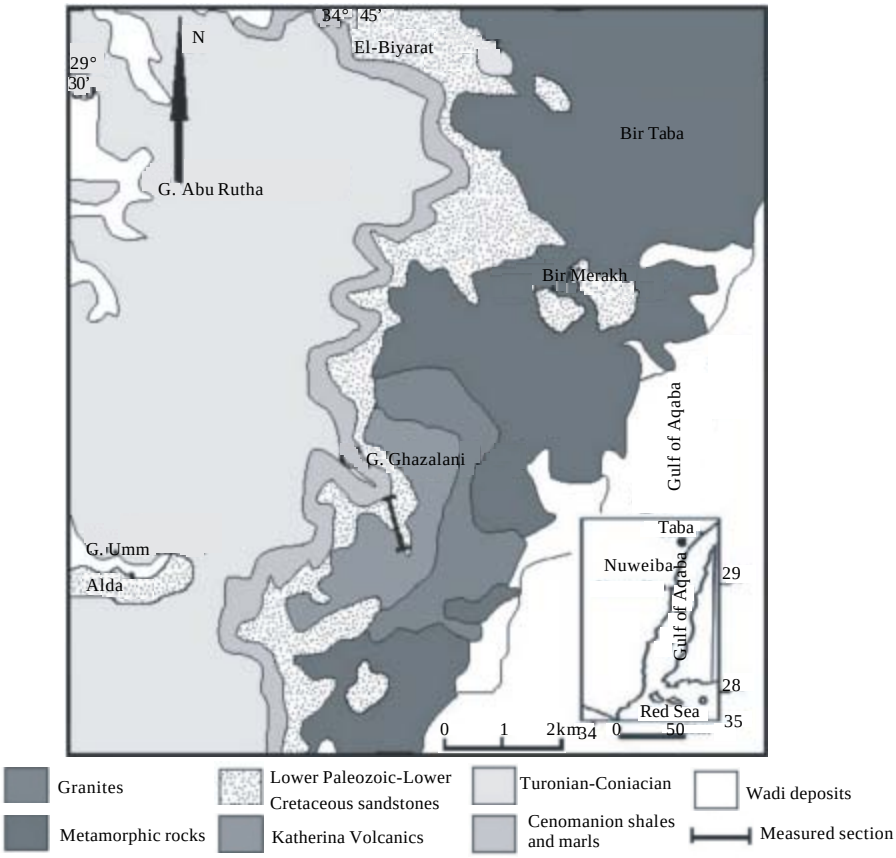

Fig. 1: Geologic map of Gebel Ghazalani area (Klitzsch *et al.* (1986) with modifications)

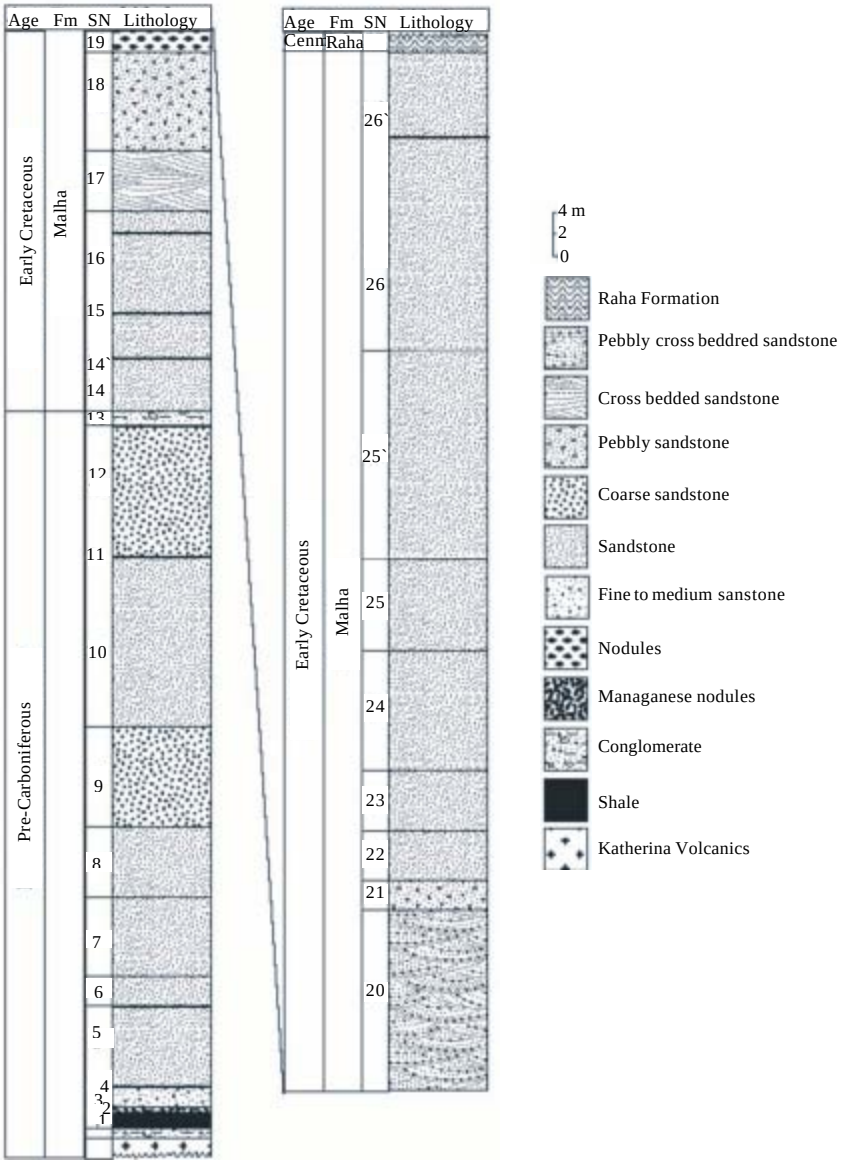

Fig. 2: Lithostratigraphy of the studied pre-Cenomanian succession in G. Ghazalani area

succession a major unconformity is evidenced between the Paleozoic and the Early Cretaceous. The studied sequence can be distinguished, from base to top into: undifferentiated Paleozoic (pre-Carboniferous) and Lower Cretaceous well-documented Malha Formation (Fig. 2). The sandstone of the pre-Carboniferous (Kostandi, 1959; Said, 1962; Akarish, 1998) section (~72 m thick) unconformably overlies the Katherina Volcanics and underlies the Lower Cretaceous Malha Formation. It is formed of unfossiliferous semi-hard to friable sandstones intercalated with yellow clay layers in the lower part. The sandstones have various colors ranging from yellow to brown and sometimes white. They are mainly fine to medium in grain size.

On the other hand, the sandstones of the Malha Formation (Abdallah and El-Adindani, 1963) underlie the Cenomanian shales and marls without break in sedimentation and its lower contact with the underling pre-Carboniferous sediments is marked by 1.5 m thick conglomerate bed formed of quartz and other basement gravels embedded into kaolinitic sandstone matrix. A paleosol layer ~0.50 m thick is present on the top of the conglomerate bed. Similar features were described at Sheikh Attia area (Issawi *et al*., 1999). Lithologically, the

Malha Formation (~140 m thick) is formed of monotonous/thickly bedded medium-grained sandstones with subordinate pebbly sandstone beds with stringers of pebbles. The sandstones are hard to semi-hard with various colors ranging from white to yellow and brown. They are medium-grained exhibiting upward fining and showing common cross-bedding and are intercalated by green to grey and yellow clay rich beds, mainly in the lower part.

EXPERIMENTAL

Data collection and analysis: A total of thirty samples were collected from the pre-Cenomanian sedimentary succession exposed at G. Ghazalani area in East Sinai representing the different encountered lithologies. X-Ray Diffraction (XRD) analysis was carried out on the <2 μm of the clay fraction separated from the sandstones and the clay rich samples. Three oriented mounts of clay fractions (<2 μm) were examined, namely air-dried, slurried in ethylene glycol and heated at 550°C for 2 h (Tucker, 1988). The obtained diffraction data were interpreted using the ASTM (American Standard for Testing and Materials) cards together with the data published by Brindley (1961). Geochemical investigations based on the data of major, trace and rare earth elements were carried out. A total of 17 samples were chemically analyzed for their major element concentration using X-Ray Fluorescence Spectrometry at Saudi Geological Survey, Jeddah, Saudi Arabia. While trace and rare earth element concentrations were determined in 10 selected samples in Acme analytical Laboratory LTD., Vancouver, Canada. The analyses were carried out by both Induced Coupled Plasma-Mass Spectrometry (ICP-MS) and Induced Coupled Plasma-Emission Spectrometry (ICP-ES).

RESULTS AND DISCUSSION

Clay mineralogy: The clay fraction mineralogy of the concerned sandstones shows that the clay minerals are mainly represent by kaolinite as sole mineral or by mixture of kaolinite and rare illite. Kaolinite is identified by its basal reflections at d-spacing: 7.14, 3.56 and 2.35Å. These reflections were not affected by glycolation while removed out upon heating at 550°C for 2 h. Their sharpness and intensities reflect moderate crystallinity. Illite is identified by the most intense peaks at 10.04 and 4.95 Å which were neither affected by heating nor glycolation. The prevalence of kaolinite with minor or without illite indicates their sedimentary origin under continental weathering conditions in non-marine environment (Lonnie, 1982). The moderate crystallinity gained by most of kaolinites suggests that they are chiefly of detrital inheritance and are relate to fluvial environment (Keller, 1956; Abu-Zeid *et al*., 1991). This refers to their direct derivation from weathering horizons and/or soils on sedimentary and quartz-bearing plutonic rocks.

Geochemistry

Major elements: Bulk geochemistry of the major elements of 17 pre-Cenomanian samples from Gebel Ghazalani area are given in Table 1. Major element distribution patterns reflect the mineralogy of the studied samples. The sandstone samples have lower Al_2O_3 contents than the associated fine-grained mud enriched samples (samples 1, 4, 11 and 15). Most of these associated "mudstones" are enriched in Al_2O_3, K_2O, Fe_2O_3 and TiO_2 in comparison with the sandstones, reflecting their higher content in clay. In general, the pre-Cenomanian sandstones are rich in SiO_2 contents between 74.55 and 98.3% with an average 91.74% i.e. quartz-rich following the criteria of Crook (1974). They possess low contents of TiO_2 and Fe_2O_3, the alkali and alkaline oxides. Generally, low concentrations of Fe_2O_3 and TiO_2 in all sandstones reflect low abundances of Ti-bearing minerals (biotite, ilmenite, titanite and titaniferous magnetite) in the analyzed samples (Armstrong-Altrin *et al*., 2004). MnO and P_2O_5 are strongly depleted and there are no significant differences in the contents of MnO and P_2O_5 among the samples.

By comparison with the average Upper Continental Crust (UCC) and post Archean Australian Average Shale (PAAS), representative continentally derived sediments, values of Taylor and McLennan (1985), the pre-Cenomanian sandstones are enriched in SiO_2 but, are depleted in all other major elements (Fig. 3). The observed depletion in Na_2O, MnO and CaO is not only likely due to quartz dilution but also indicates that the studied sediments have been suffered from intense weathering and recycling (Joo *et al*., 2005; Jin *et al*., 2006). Generally, Ca, Na and K contents are controlled by feldspars and thus strong depletion in CaO, Na_2O further suggests destruction of plagioclase due to chemical weathering in the source or during transport. SiO_2 content has a strong negative correlation with Al_2O_3 content ($r = -1$; Fig. 4g) reflecting that much of SiO_2 is present as quartz grains. Low values of Al_2O_3/SiO_2 (range = 0.01-0.22; average = 0.06; Table 1) confirm the quartz enrichment in the studied sandstones. With the exception of SiO_2, the other oxides broadly follow the trend of Al_2O_3 (Fig. 4), indicating that they are associated with micaceous and/or clay minerals in the sediments. Plotting of Al_2O_3 (Fig. 4) vs. major oxides variation diagrams, Fe_2O_3, MnO, MgO, CaO, Na_2O and K_2O show positive correlation. This

Table 1: Major element concentrations (wt.%) of pre-Cenomanian sandstones in G. Ghazalani

Elements	1	3	4	7	8	10	11	12	15	16	20	21	22	23	24	25	26	Average	UCC	PAAS
SiO_2	78.12	98.30	84.33	96.05	96.90	96.70	82.85	97.57	74.55	96.40	92.48	94.60	97.10	92.60	91.40	97.60	92.00	91.74	66.00	62.80
Al_2O_3	13.40	0.70	9.80	1.42	0.88	1.54	9.80	1.07	16.60	1.69	4.67	3.32	1.26	3.80	4.96	1.36	5.00	4.78	15.20	18.90
TiO_2	0.35	0.05	1.19	0.08	0.06	0.10	1.06	0.07	1.69	0.11	0.32	0.16	0.07	0.16	0.19	0.08	0.14	0.35	0.50	1.00
Fe_2O_3	0.28	0.10	0.20	0.05	0.47	0.10	0.28	0.07	0.78	0.10	0.42	0.17	0.09	0.29	0.47	0.06	0.19	0.24	5.00	7.22
MnO	0.02	0.00	0.05	0.03	0.00	0.03	0.05	0.00	0.04	0.00	0.02	0.01	0.01	0.03	0.04	0.00	0.01	0.02		0.11
CaO	0.21	0.14	0.17	0.15	0.09	0.09	0.85	0.10	0.05	0.21	0.13	0.09	0.06	0.05	0.07	0.09	0.10	0.16	4.20	1.30
MgO	0.10	0.12	0.09	0.07	0.08	0.05	0.11	0.06	0.09	0.09	0.10	0.08	0.03	0.06	0.05	0.07	0.06	0.08	2.20	2.20
Na_2O	0.51	0.07	0.05	0.19	0.03	0.08	0.07	0.04	0.14	0.05	0.05	0.08	0.05	0.07	0.08	0.07	0.07	0.10	3.90	1.20
K_2O	0.09	0.08	0.11	0.06	0.05	0.09	0.24	0.05	0.29	0.07	0.10	0.06	0.06	0.08	0.12	0.09	0.51	0.13	3.40	3.70
P_2O_5	0.05	0.01	0.05	0.02	0.01	0.01	0.04	0.03	0.05	0.01	0.02	0.02	0.05	0.03	0.01	0.03	0.03	0.03		0.16
L.O.I.	6.75	0.70	3.55	1.54	0.88	1.05	4.30	0.64	5.33	0.76	1.75	1.27	0.90	1.65	1.65	0.39	1.68	2.05		
Total	99.88	100.27	99.59	99.66	99.45	99.84	99.65	99.70	99.61	99.49	100.06	99.86	99.68	98.82	99.04	99.84	99.79	99.66		
CIA	91.03	60.52	95.05	68.56	76.70	79.67	83.61	77.99	96.31	75.78	91.62	90.20	83.08	92.84	92.72	78.32	85.48	83.50		
PIA	91.58	62.37	96.11	69.80	79.49	82.99	85.17	80.39	98.06	77.66	93.47	91.67	86.18	94.73	94.91	81.89	93.73	85.90		
CIW	91.63	65.42	96.16	70.78	80.50	83.89	85.51	81.19	98.10	78.45	93.61	91.82	86.80	94.85	95.03	82.97	94.39	86.54		
SiO_2/Al_2O_3	5.83	140.43	8.61	67.64	110.11	62.79	8.45	91.19	4.49	57.04	19.80	28.49	77.06	24.37	18.43	71.76	18.4	47.94		
Al_2O_3/SiO_2	0.17	0.01	0.12	0.01	0.01	0.02	0.12	0.01	0.22	0.02	0.05	0.04	0.01	0.04	0.05	0.01	0.05	0.06		
K_2O/Al_2O_3	0.01	0.11	0.01	0.04	0.06	0.06	0.02	0.05	0.02	0.04	0.02	0.02	0.05	0.02	0.02	0.07	0.10	0.04		
Al/Na**	15.92	6.06	118.79	4.53	17.78	11.67	84.85	16.21	71.86	20.48	56.61	25.15	15.27	32.90	37.58	11.77	43.29	34.75		
Al/K**	137.55	8.08	82.31	21.86	16.26	15.81	37.72	19.77	52.88	22.30	43.14	51.12	19.40	43.88	38.19	13.96	9.06	37.25		
K/Na**	0.12	0.75	1.44	0.21	1.09	0.74	2.25	0.82	1.36	0.92	1.31	0.49	0.79	0.75	0.98	0.84	4.78	1.16		
Ti/Na**	0.53	0.55	18.41	0.33	1.55	0.97	11.71	1.35	9.34	1.70	4.95	1.55	1.08	1.77	1.84	0.88	1.55	3.53		
Rb/K**	12.25		25.05			19.59	41.33		39.90	50.38	33.06		20.21		50.51		35.01	32.73		

CIA: Chemical index of alteration, PIA: Plagioclase index of alteration, CIW: Chemical index of weathering, ** Molar ratios. UCC: Average upper continental crust (Taylor and McLennan, 1985), PAAS: Post-Archean average Australian Shale (Taylor and McLennan, 1985)

suggests that most oxides including CaO are resulting chiefly from aluminosilicates (Jin *et al*., 2006). Using the geochemical classification diagram of Herron (1988), G. Ghazalani sandstones are represented chiefly by quartz arenites with few litharenite and sublitharenite and rare wackes, indicating relatively mature sediments. This interpretation agrees with petrographic data from correlative (pre-Cenomanian) strata in Central Sinai (Salem *et al*., 2001) that were regarded as mineralogically mature sandstones.

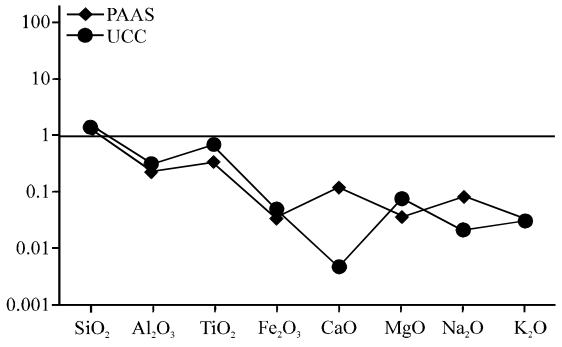

Fig. 3: Spider plot of average major element contents for G. Ghazalani sandstones normalized against PAAS and UCC, data are after Taylor and McLennan (1985)

Trace elements: The trace element contents of 10 selected sandstone samples from G. Ghazalani are given in Table 2. The normalized trace element averages of the studied sediments with respect to the average UCC and PAAS (Taylor and McLennan, 1985) are shown in the spider diagram Fig. 5; in this diagram, the normalized trace elements are arranged in order of decreasing compatibility in typical igneous differentiation series. Most compatible elements are shown to the left followed by incompatible elements towards the right along the X-axis (Ghosh and Sarkar, 2010).

The main feature of the trace element distributions is the generally positive correlation with Al_2O_3, reflecting association of most elements with the clay fraction. The studied sandstones have low concentrations of the transition metals Co, Ni and V. These elements are

Table 2: Trace-element concentrations (ppm) for sandstones of G. Ghazalani

No.	1	4	10	11	15	16	20	22	24	26	Average	UCC	PAAS
Ba	24.00	97.00	11.00	62.00	96.00	26.00	43.00	22.00	20.00	90.00	49.10	550.00	650.00
Be	2.00	1.00	1.00	2.00	3.00	1.00	1.00	1.00	1.00	1.00	1.40	3.00	
Co	3.50	1.60	0.90	2.50	2.40	1.50	1.10	0.70	2.10	3.30	1.96	10.00	23.00
Cs	0.10	0.10	0.20	0.40	0.90	0.30	0.20	0.10	0.40	0.70	0.34	3.50	15.00
Ga	29.40	18.00	3.50	14.50	20.50	3.60	4.20	1.90	6.00	5.40	10.70	17.00	20.00
Hf	19.30	49.00	9.90	37.60	21.60	3.90	8.50	1.10	1.90	3.90	15.67	5.80	5.00
Nb	43.00	54.20	2.90	31.20	37.50	4.00	7.30	1.90	3.90	4.40	19.03	25.00	19.00
Rb	1.00	2.50	1.60	9.00	10.50	3.20	3.00	1.10	5.50	16.20	5.36	112.00	160.00
Sn	7.00	4.00	1.00	3.00	3.00	1.00	1.00	1.00	1.00	1.00	2.30	5.50	
Sr	36.40	372.20	10.80	114.00	136.00	22.60	45.00	22.50	27.00	24.00	81.05	350.00	200.00
Ta	2.40	3.80	0.30	2.40	2.50	0.30	0.60	0.10	0.30	0.30	1.30	2.20	
Th	13.20	27.50	1.80	13.80	13.70	2.00	2.80	0.90	2.00	2.80	8.05	10.70	14.60
U	5.10	8.50	0.80	6.80	4.90	0.70	1.00	0.30	0.70	1.20	3.00	2.80	3.10
V	15.00	77.00	9.00	72.00	80.00	14.00	18.00	8.00	18.00	17.00	32.80	60.00	150.00
W	1.70	6.70	5.00	4.50	7.60	0.90	1.50	5.00	2.90	5.00	4.08	2.00	2.70
Zr	760.10	1822.00	382.10	1387.00	783.60	152.40	321.80	37.10	68.80	135.80	585.07	190.00	210.00
Y	78.30	82.80	6.10	41.90	35.40	6.30	10.00	3.00	7.10	16.70	28.76	22.00	27.00
Cu	84.80	49.40	13.60	35.70	68.20	8.70	12.90	8.80	5.20	6.80	29.41	25.00	50.00
Pb	3.90	10.30	1.30	9.80	14.40	2.00	1.30	0.80	1.20	3.10	4.81	20.00	20.00
Zn	29.00	10.00	6.00	11.00	29.00	8.00	11.00	3.00	13.00	24.00	14.40	71.00	85.00
Ni	5.50	1.50	1.20	2.50	4.40	2.20	2.20	0.80	3.80	4.40	2.85	20.00	55.00
Ag	2.40	1.40	2.50	1.10	2.50	2.30	1.90	1.70	2.00	3.80	2.16		
Au	13.80	1.90	1.40	1.00	0.60	0.50	2.20	1.20	1.00	0.50	2.41		
U/Th	0.39	0.31	0.44	0.49	0.36	0.35	0.36	0.33	0.35	0.43	0.38	0.26	0.21
Th/U	2.59	3.24	2.25	2.03	2.80	2.86	2.80	3.00	2.86	2.33	2.67	3.82	4.71
Th/Co	3.77	17.19	2.00	5.52	5.71	1.33	2.55	1.29	0.95	0.85	4.12	1.07	0.63
Th/Yb	1.81	3.03	2.54	2.96	3.47	3.33	2.57	3.46	2.74	2.26	2.82	4.86	5.21
Th/Tb	6.53	12.39	15.00	14.53	13.17	10.53	9.66	10.00	5.41	4.83	10.20		
La/Co	11.69	48.56	5.22	11.20	16.04	4.27	6.91	4.86	5.29	4.03	11.81	3.00	1.65
La/Th	3.10	2.83	2.61	2.03	2.81	3.20	2.71	3.78	5.55	4.75	3.34	2.80	2.60
La/Ni	7.44	51.80	3.92	11.20	8.75	2.91	3.45	4.25	2.92	3.02	9.97	1.50	0.69
Zr/Co	217.17	1138.75	424.56	554.80	326.50	101.60	292.55	53.00	32.76	41.15	318.28		
Zr/Nb	17.68	33.62	131.76	44.46	20.90	38.10	44.08	19.53	17.64	30.86	39.86	7.60	11.05
Zr/Th	57.58	66.25	212.28	100.51	57.20	76.20	114.93	41.22	34.40	48.50	80.91	17.76	14.38
Ti/Zr	2.76	3.92	1.57	4.59	12.94	4.33	5.97	11.32	16.57	6.19	7.02	15.79	14.29
Ba/Co	6.86	60.63	12.22	24.80	40.00	17.33	39.09	31.43	9.52	27.27	26.92	55.00	28.26

PAAS: Post-archean average Australian shale (Taylor and Mclennan, 1985) and UCC: Average upper continental crust (Talyor and Mclennan, 1985)

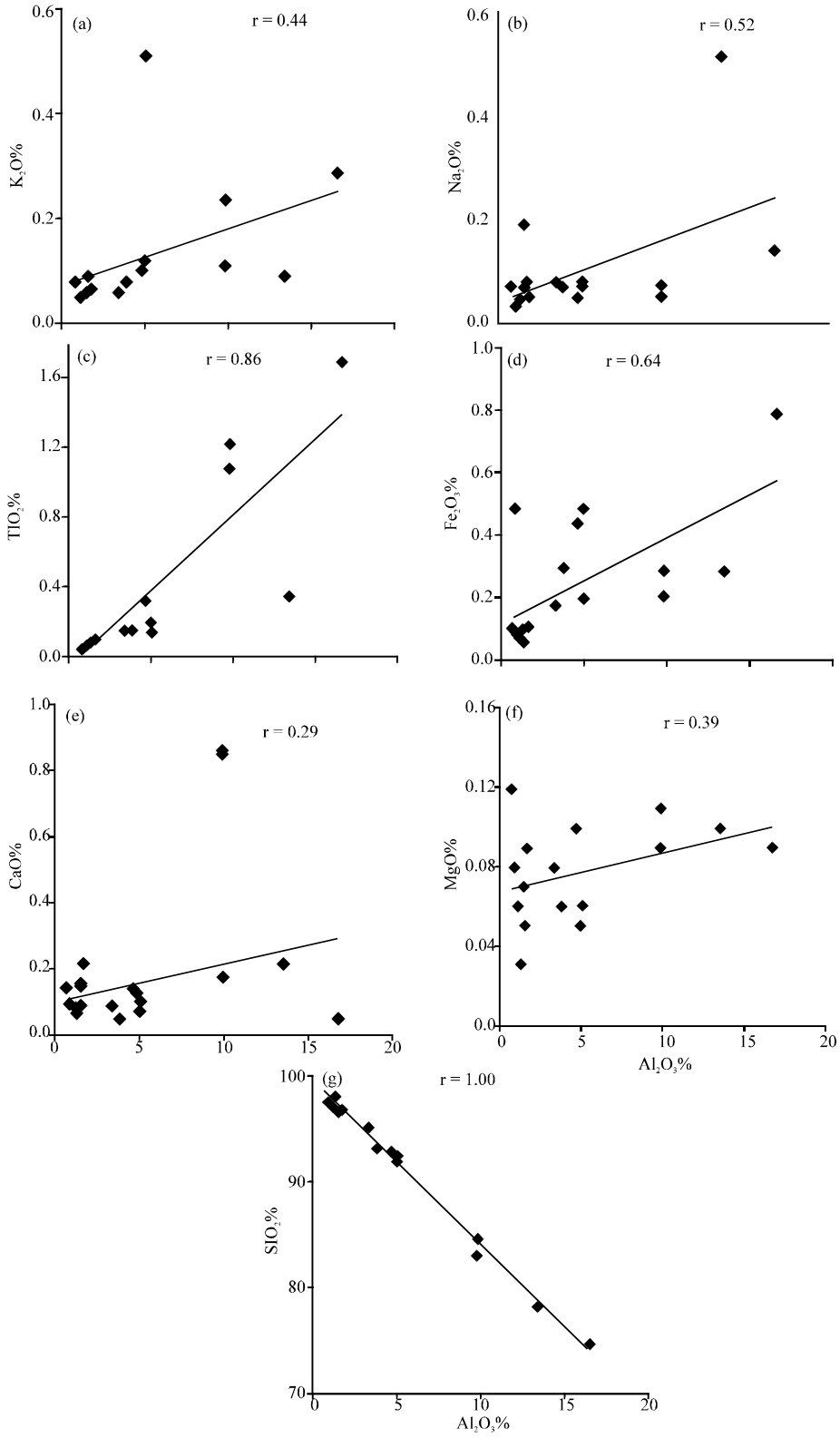

Fig. 4(a-g): Co-variation of Al_2O_3 vs. major elements for G. Ghazalani sandstones. Notice the positive correlation of Al_2O_3 with the major elements, SiO_2 shows negative correlation

strongly depleted in respect to UCC and PAAS. Cu is slightly enriched relative to UCC and depleted to PAAS. Depletion of these elements may indicate the negligible role of the basic rocks as a source rocks. These elements are mainly concentrated in the clays or metal oxides (Turekian and Michael, 1960). Vanadium is positively correlated with Fe_2O_3 (r = 0.49) and TiO_2 (r = 0.97). It is generally adsorbed on kaolinite and possibly associated with iron oxide minerals (Hirst, 1962). Positive correlations of Co, Ni, Zn, Cu and V with both Fe_2O_3 (r = 0.29, 0.53, 0.59, 0.42 and 0.49, respectively, Fig. 6) and Al_2O_3 (r = 0.63, 0.63, 0.77, 0.91 and 0.72, respectively, Fig. 7) also indicate that these elements are linked with iron oxides and clay minerals.

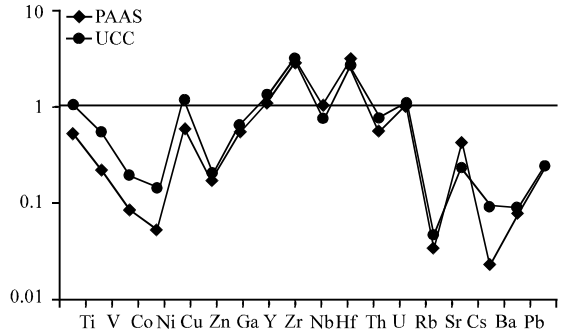

Fig. 5: PAAS, UCC-normalized averages trace element concentrations for G. Ghazalani sandstones. PAAS and UCC data are after Taylor and McLennan (1985)

In general, the studied sandstones have significantly Low Large-Ion Lithophile Elements (LILE), Ba, Cs, Rb, Pb and Sr concentrations. These elements are highly depleted comparable to those of Upper Continental Crust (UCC) and PAAS (Fig. 5). Depletions of LILE may reflect intense weathering and recycling. Low Sr content is generally related to low CaO content, probably due to the lack of calcic plagioclase.

Rare Earth Elements (REE): The results of REE analyses are listed in Table 3 and are shown as chondrite-normalized patterns in Fig. 8. Total REE (ΣREE) abundances are variable throughout the succession (Table 3). Pre-Cenomanian sandstones have a wide range of total REE (ΣREE) contents of 17.4-419.47 ppm with an average 133.43 ppm (Table 3) which is

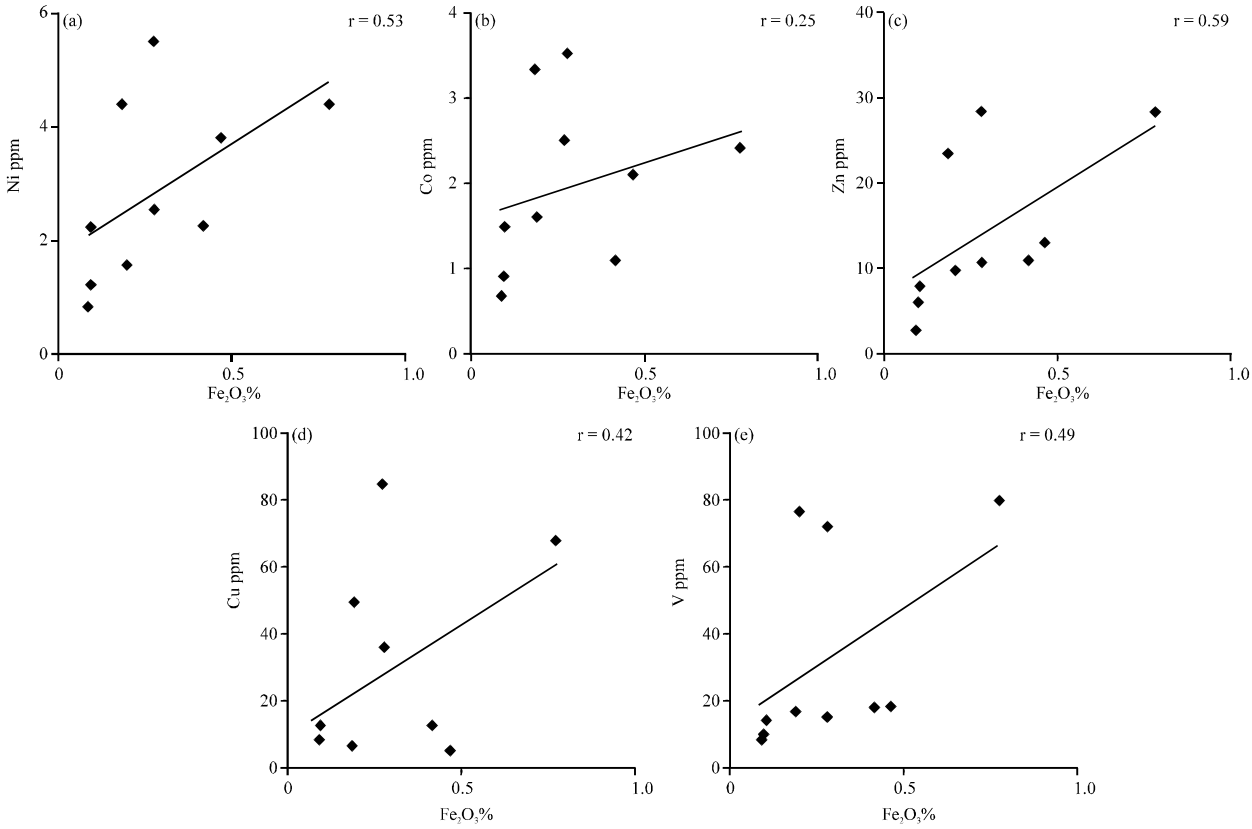

Fig. 6(a-e): Plots of Fe_2O_3 against (a) Ni, (b) Co, (c) Zn, (d) Cu and (e) V for G. Ghazalani sandstones

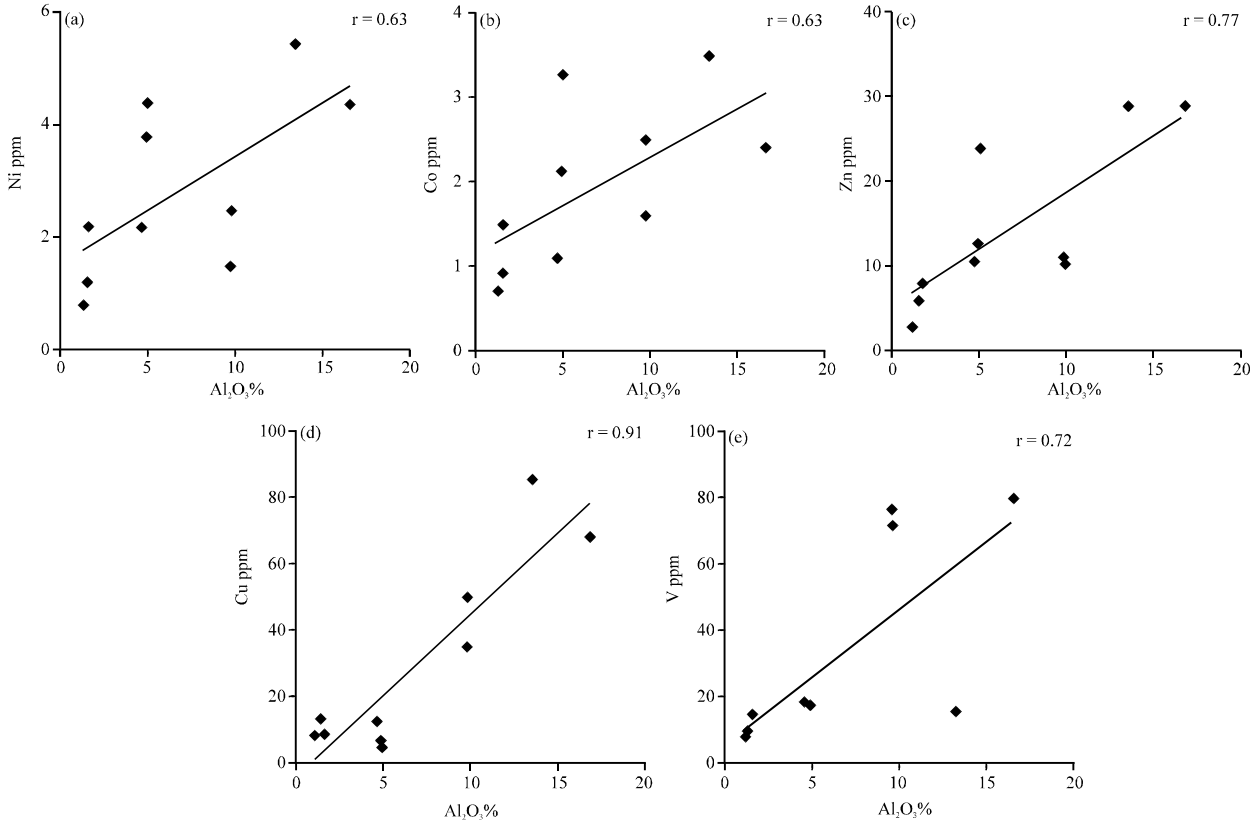

Fig. 7(a-e): Plots of Al_2O_3 against (a) Co, (b) Ni, (c) Zn, (d) Cu and (e) V for G. Ghazalani sandstones

Table 3: Rare earth element concentrations (ppm) of pre-Cenomanian sandstones in G. Ghazalani

No.	1	4	10	11	15	16	20	22	24	26	Average	UCC	PAAS
La	40.90	77.70	4.70	28.00	38.50	6.40	7.60	3.40	11.10	13.30	23.16	30.00	38.00
Ce	125.00	172.30	10.10	57.10	82.60	14.70	18.00	7.50	31.60	36.40	55.53	64.00	80.00
Pr	13.47	18.92	1.12	6.01	8.83	1.68	2.17	0.84	4.12	4.50	6.17	7.10	8.90
Nd	53.80	79.60	3.90	22.50	32.90	7.00	9.30	3.10	16.70	20.80	24.96	26.00	32.00
Sm	10.93	16.60	0.73	4.50	6.50	1.33	1.91	0.61	3.55	4.21	5.09	4.50	5.60
Eu	0.92	3.24	0.14	0.95	1.45	0.29	0.46	0.12	0.76	0.91	0.92	0.88	1.10
Gd	11.06	13.58	0.78	4.69	5.83	1.11	1.80	0.58	2.63	3.78	4.58	3.80	4.70
Tb	2.02	2.22	0.12	0.95	1.04	0.19	0.29	0.09	0.37	0.58	0.79	0.64	0.77
Dy	12.40	12.36	0.86	5.87	5.87	1.01	1.66	0.45	1.68	3.03	4.52	3.50	4.40
Ho	2.64	2.71	0.20	1.34	1.23	0.20	0.34	0.10	0.28	0.55	0.96	0.80	1.00
Er	7.97	8.48	0.55	4.19	3.73	0.57	1.03	0.27	0.73	1.47	2.90	2.30	2.90
Tm	1.13	1.28	0.08	0.65	0.55	0.09	0.15	0.04	0.10	0.21	0.43	0.33	0.40
Yb	7.28	9.07	0.71	4.67	3.95	0.60	1.09	0.26	0.73	1.24	2.96	2.20	2.80
Lu	1.14	1.41	0.11	0.77	0.63	0.10	0.18	0.04	0.11	0.18	0.47	0.32	0.43
LREE	244.10	365.12	20.55	118.11	169.33	31.11	38.98	15.45	67.07	79.21	114.90	131.60	164.50
HREE	44.50	49.70	3.30	22.36	22.20	3.77	6.36	1.79	6.52	10.86	17.14	13.57	16.97
LREE/HREE	5.49	7.35	6.23	5.28	7.63	8.25	6.13	8.63	10.29	7.29	7.26	9.70	9.69
∑REE	290.66	419.47	24.10	142.19	193.61	35.27	45.98	17.40	74.46	91.16	133.43	146.37	183.00
Gd_n/Yb_n	1.23	1.21	0.89	0.81	1.20	1.50	1.34	1.81	2.92	2.47	1.54	1.40	1.36
La_n/Lu_n	3.72	5.72	4.44	3.78	6.34	6.64	4.38	8.82	10.48	7.67	6.20	9.73	9.17
La_n/Sm_n	2.36	2.95	4.05	3.92	3.73	3.03	2.50	3.51	1.97	1.99	3.00	4.20	4.27
Eu/Eu*	0.26	0.66	0.57	0.63	0.72	0.73	0.76	0.62	0.76	0.70	0.64	0.65	0.66
Ce/Ce*	1.25	1.05	1.03	1.03	1.05	1.05	1.04	1.04	1.09	1.10	1.07	1.03	1.02

$Eu/Eu^* = Eu_N/(Sm_N \times Gd_N)^{0.5}$ and $Ce/Ce^* = Ce_N/(La_N \times Pr_N)^{0.5}$, where subscript n indicates normalization to chondrite. PAAS: Post-archean average Australian Shale (Taylor and Mclennan, 1985) and UCC: Average upper continental crust (Talyor and Mclennan, 1985)

relatively close to that of the UCC (Taylor and McLennan, 1985). The associated mud rich beds have greater REE abundances (ΣREE contents of 142-419 ppm with an average about 261 ppm) than sandstones, suggesting that clays control the REE distributions (Hossain *et al*., 2010). The good positive correlation between Al_2O_3 and the REE contents confirms that the REE are mostly concentrated in the fine fractions (clay). Generally, the ΣREE contents

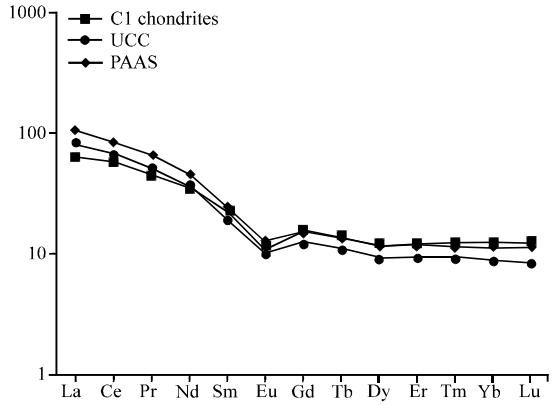

Fig. 8: Chondrite-normalized averages REE patterns of G. Ghazalani sandstones. The PAAS and UCC patterns are given as a reference; data are after Taylor and McLennan (1985)

are less than 200 ppm that may reflect quartz dilution. Values are lower in the sandstones having higher SiO_2 contents. In general, chondrite-normalized REE patterns for the studied sandstone from G. Ghazalani (Fig. 8) are characterized by high light REE/heavy REE (LREE/HREE) ratio (5.28-10.29, Table 3), flat HREE pattern and pronounced negative Eu anomaly. LREEs are fractionated, $(La/Sm)_n$ = 3.00 and the HREE patterns are almost flat, $(Gd/Yb)_n$ = 1.54. This chondrite-normalized pattern is typical of sediments and sedimentary rocks enrichment in light REE (LREE), flat heavy REE (HREE) and negative Eu anomaly (Borges *et al*., 2008). The chondrite-normalized REE patterns for Gazalani sandstones (Fig. 8) are similar to that displayed by upper continental crust and PAAS (Taylor and McLennan, 1985) but the LREEs are slightly similar relative to UCC and slightly depleted relative to PAAS. (HREE) are nearly typical to PAAS and enriched relative to UCC, this may be due to higher concentration of heavy minerals especially zircon which has a high concentration of HREE (Taylor and McLennan, 1985; Lee, 2002). The europium anomaly of Gazalani sandstones is always negative, ranging from 0.26 to 0.76 (average 0.64) which is quite typical to that of UCC (0.65) and PAAS (0.66).

TECTONIC SETTING

Bhatia (1983) and Roser and Korsch (1986) used the chemical composition of sandstones to investigate provenance and tectonic setting of sedimentary rocks. Roser and Korsch (1986) introduced a discrimination diagram utilizing log (K_2O/Na_2O) versus SiO_2 to determine the tectonic setting of terrigenous

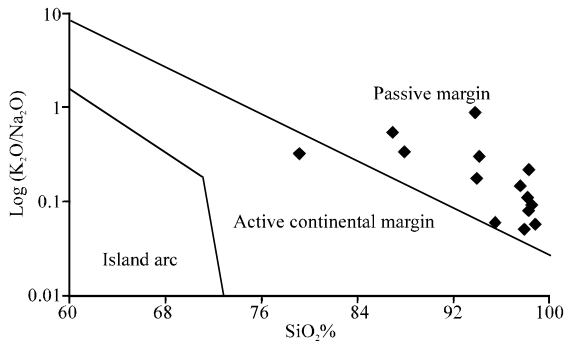

Fig. 9: K_2O/Na_2O-SiO_2 relations for G. Ghazalani sandstones, data recalculated to 100% volatile free, tectonic setting fields are after Roser and Korsch (1986)

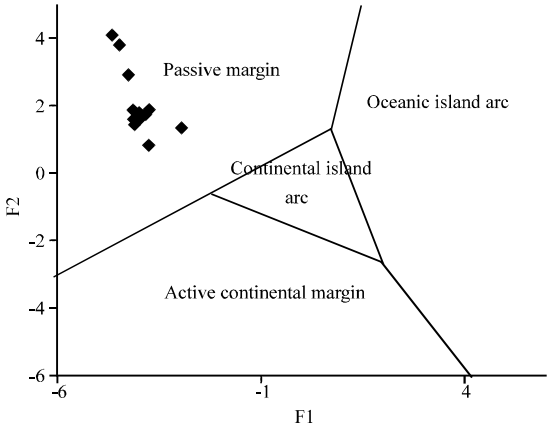

Fig. 10: Discrimination function plot of G. Ghazalani sandstones, data recalculated to 100% volatile free, tectonic setting fields are after Bhatia (1983)

sedimentary rocks. Both SiO_2 and log (K_2O/Na_2O) values increase from volcanic arc to active-continental-margin to passive margin settings that signify continentally derived sediments distinct by high SiO_2 and low Na_2O. The plot K_2O/Na_2O versus SiO_2 for the study samples (Fig. 9) implies that they are typical of sediments deposited in passive margin setting. According to Roser and Korsch (1986), passive margin sediments are largely quartz-rich sediments derived from plate interiors or stable continental areas and deposited in intracratonic basins or on passive continental margins. Discrimination of tectonic settings based on major elements also was proposed by Bhatia (1983); it includes oceanic island arc, continental island arc, active continental margin and passive margin. Plotting the studied sandstones on this discriminant function, all samples fall deeply in the area of passive setting (Fig. 10). According to Asiedu *et al.* (2005), clastic

Table 4: Range of elemental ratios of Gebel Ghazalani sediments compared to the ratios derived from silicic and basic sources

Element ratio	Range of G. Ghazalani sediments		Rang of sediments from silicic sources[1]		Range of sediments from basic sources[1]	
Eu/Eu *	0.26-0.76		0.40-0.94		0.71-0.95	
$(La/Lu)_N$	3.72-10.48		3.00-27.00		1.10-10.00	
La/Co	4.03-48.56		1.8-13.8		0.14-0.38	
Th/Co	0.85-17.19		0.67-19.4		0.04-.4	
	Gebel Ghazalani sediments		Active continental margin[2]		Passive continental margin[2]	
	Average	Range	Average	Range	Average	Range
Ti/Zr	7.02	1.57-16.57	15.3	10-35	6.74	<10
			Oceanic island arc[2]		Continental island arc[2]	
			Average	Range	Average	Range
Ti/Zr			56.8	>40	19.7	10-35

[1]Cullers (1994), Cullers (2000), Cullers and podkovyrov (2000), Cullers *et al.* (1988). [2]Bhatia and Crook (1986)

rocks deposited in cratonic basins and passive margins, as in the case of the present study, are basically mature sediments, mainly quartz arenites and shales indicating deep weathering, low relief in source areas and prolonged transport across quiet continental surfaces.

According to the Th-Co-Zr/10 plot (Bhatia and Crook, 1986), the Pre- Cenomanian sediments lie in or close to the passive margin field; plot of samples close to Zr/10 apex reflects the enrichment of Zr.

Sediments of passive margin tectonic setting are characterized by low Ti/Zr ratio (generally less than 10), compared to the other tectonic settings (Bhatia and Crook, 1986). Ghazalani sandstones have Ti/Zr ratio (average ~7; Table 2) which is close to the Ti/Zr ratio (average = 6.74) estimated by Bhatia and Crook (1986) for the sediments deposited in passive margin setting (see latter Table 4). Negative Sr anomaly as shown by the studied sandstone (Fig. 5) is an indication of old recycled environments passive continental margin settings (Mader and Neubauer, 2004; Ghosh and Sarkar, 2010).

G. Ghazalani sediments deposited in the passive margin setting are resemble to those of the Atlantic type sediments and can be categorized by higher Zr contents, higher Zr/Nb, Zr/Th ratios and lower Rb, V and Ti/Zr ratio. These features mirror the recycling of these sediments, the depletion of feldspar and labile fragments and the increased abundance of heavy minerals, mainly zircon, through sedimentary processes.

PROVENANCE

Major elements, trace elements and the REE were used to infer the provenance of sandstones. Several trace and REE were expected to be more useful in discriminating source rock compositions and tectonic setting due to their relatively low mobility during sedimentary processes and their short residence times in seawater (Taylor and McLennan, 1985). These elements are probably transferred quantitatively into clastic sediments during weathering and transportation, reflecting the signature of the parent materials (Bhatia and Crook, 1986; McLennan, 1989).

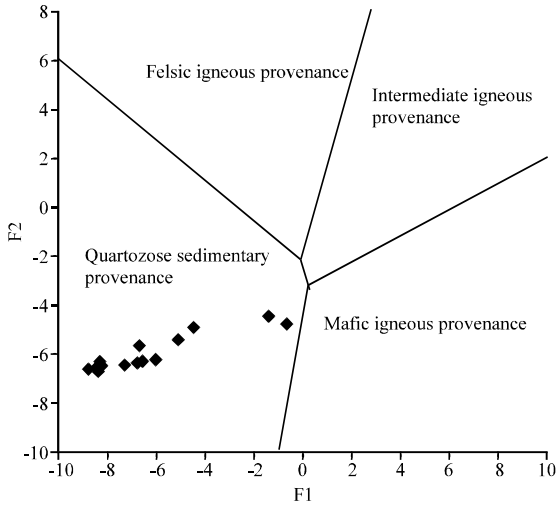

Fig. 11: Discriminant function diagram using major elements, Provenance fields are after Roser and Korsch (1988)

Roser and Korsch (1988) used major element discriminant functions to discriminate four provenances, namely mafic (P1), intermediate (P2), felsic (P3) and quartzose recycled (P4). Plotting the present data in this diagram, all the samples fall deeper within the P4 field (Fig. 11). This supports the interpretation that they were derived from granitic to gneissic or from a sedimentary source area (Roser and Korsch, 1988). Position of the studied samples deep into the P4 field is similar to that observed for several recycled suites elsewhere (Roser *et al.*, 1996).This was interpreted as the effect of recycling, with progressive loss of feldspar and relative increase in quartz. The deeper plot position of G. Ghazalani samples may therefore reflect more advanced weathering and maturation in these fluvial sediments. This observation clearly indicates the less possibility of the mafic rocks as source rocks for the studied samples of the pre-Cenomanian (Nagarajani *et al.*, 2007).

Transition metal elements (Co, Cu, Ni and V) are well-suited in magmatic processes and therefore they are

highly concentrated in mafic and ultramafic rocks than felsic igneous source rocks and their weathered products. In addition, these elements are relatively immobile through weathering. They are supposed to be transported completely in the terrigenous component of sediment and thus mirror the chemistry of their source rocks (McLennan *et al*., 1980; Armstrong-Altrin *et al*., 2004). The significant low concentration of Co, Cu, Ni and V in the studied sandstones and their strong depletion relative to PAAS (Fig. 5) can be interpreted as the result of sediment derivation from a slightly more silicic and fractionated source than the PAAS. Also, relative contribution of mafic/felsic (granitoids) sources can be reflected by the Ba/Co ratio, as these elements are largely contained in K-bearing and ferromagnesian minerals, respectively (Taylor and McLennan, 1985; Cullers *et al*., 1988). The pre-Cenomanian sediments have elevated Ba contents but are depleted in Co. The higher Ba/Co ratio (Table 2) is an indication of sediments derived from weathered felsic-granitic sources (Cullers *et al*., 1988; Akarish and El-Gohary, 2008).

The High Field Strength Elements (HFSE) Zr, Nb, Hf, Y, Th and U are prefer initially partitioned into melts through crystallization (Feng and Kerrich, 1990) and therefore, these elements are enriched in felsic rather than mafic rocks. Along with the REE, HFSE are thought to specify compositions of provenance. In sandstones from G. Ghazalani, Nb and U have average concentration values similar to PAAS whereas Zr, Y and Hf, are slightly to highly enriched (Fig. 5). Compared to PAAS, enrichment of HFSE in G. Gazalani sandstones indicate that source rocks were more granitic in composition than those supplied detritus to PAAS (Lee, 2002).

The La/Th vs. Th/Yb and Th/Co vs. Zr/Co plots have been used to differentiate between felsic and mafic nature of source rocks (McLennan *et al*., 1980; Bhatia and Crook, 1986; Borges *et al*., 2008). In these plots (Fig. 12a, b), the studied samples show felsic character of source rocks (high Th/Co and high La/Th).

REE and Th are fairly helpful to deduce crustal compositions because their distribution is not significantly affected by secondary processes such as diagenesis and metamorphism and is less affected by heavy mineral fractionation than that for elements such as Zr, Hf and Sn (Bhatia and Crook, 1986; Armstrong-Altrin *et al*., 2004). REE and Th contents are higher in felsic than mafic igneous source rocks and in their weathered products, In addition, Eu/Eu*, $(La/Lu)_n$, Th/Co and La/Co ratios are significantly unlike in mafic and felsic source rocks and may let constraints on the provenance of sedimentary rocks (Wronkiewicz and Condie, 1989; Cullers *et al*., 1988; Cullers, 1994; Cox *et al*., 1995; Armstrong-Altrin *et al*., 2004). The Eu/Eu*, $(La/Lu)_n$, Th/Co and La/Co ratios (Table 4) of the studied pre-Cenomanian of G. Gazalani are compared with those in sediments derived from felsic and mafic source rocks (Cullers *et al*., 1988, 2000; Cullers and Podkovyrov, 2000) (Table 4). Such comparison indicates that the trace elemental ratios of this study are comparable to the range of sediments derived from felsic source rocks rather than mafic source rocks.

The relative REE patterns and Eu anomaly size have also been utilized to deduce sources of sedimentary rocks (Taylor and McLennan, 1985; Wronkiewicz and Condie, 1989). Mafic rocks contain low LREE/HREE ratios and

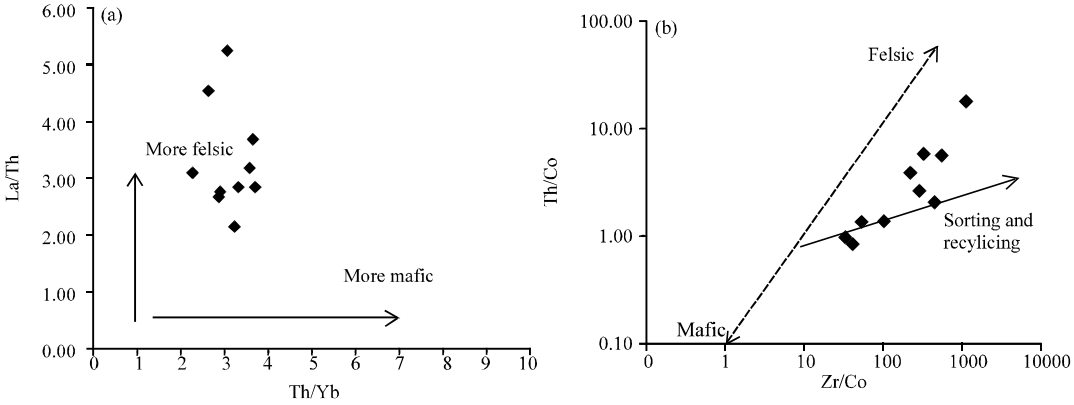

Fig. 12 (a-b): (a) La/Th vs. Th/Yb plot show felsic vs. mafic character (McLennan *et al*., 1980) and (b) Th/Co-Zr/Co plot show mafic-felsic character and recycling (McLennan *et al*., 1993). The dashed line indicates compositional difference, and deviation from this trend (solid line) represents sedimentary effects from sorting and recycling

tend not to contain Eu anomalies, whereas more felsic rocks usually contain higher LREE/HREE ratios and negative Eu anomalies (Cullers and Graf, 1984). The depletion of Eu may be interpreted as shallow, intracrustal differentiation which resulted in Eu-depletion in the upper continental crust, associated with the production of granitic rocks (McLennan, 1989). In the present study, all samples show higher LREE/HREE ratio (5.28-10.29; average 7.26; Table 3) and a significant negative Eu anomaly (0.64 Table 3; Fig. 8). Prominent negative Eu anomaly, high LREE/HREE and flat HREE pattern reflect sediment derivation from predominantly felsic rocks of the upper continental crust.

From the above mentioned trends the provenance of the studied sandstones can be explained by a sedimentary system dominated by detritus derived from recycled highly weathered silicic (granatic) materials. The trace element compositions and ratios are consistent with most sandstone being derived from a felsic (granitic) source.

SOURCE AREA WEATHERING

The intensity and duration of weathering in siliciclastic sediments can be designated through examining the relationships among alkali and alkaline earth elements (Nesbitt and Young, 1982). Since the upper crust is dominated by the presence of feldspars and volcanic glass (Nesbitt and Young, 1982, 1984), the dominant process during chemical weathering and soil formation is the degradation of labile feldspars from source rocks to secondary clay minerals. These chemical signature are ultimately transferred to sedimentary records and supply a useful means for monitoring the original composition and following weathering conditions.

The weathering history of the sources of siliciclastic sediments can be deduce through Quantitative estimation of the chemical weathering of silicates such as the calculated values of Chemical Index of Alteration (CIA), Plagioclase Index of Alteration (PIA) and Chemical Index of Weathering (CIW) (Nesbitt and Young, 1982; Fedo *et al*., 1995). Where, CIA = $Al_2O_3/(Al_2O_3+CaO^*+Na_2O+K_2O) \times 100$, PIA = $(Al_2O_3-K_2O)/(Al_2O_3+CaO^*+Na_2O-K_2O) \times 100$ and, CIW = $Al_2O_3/(Al_2O_3+CaO^*+Na_2O) \times 100$, in molecular proportions. CaO* is defined as CaO in silicates fraction only. However, in the present study there was no objective way to distinguish carbonate CaO from silicate CaO, so the detected CaO is used here. This is justified on the basis that there none of the samples is calcareous and CaO is very low (0.05-0.85, average = 0.16) (Nagarajani *et al*., 2007). Moreover, as mentioned before the detected CaO is positively correlated with Al_2O_3 implying that CaO is related only to silicates.

CIA, PIA and CIW values for G. Ghazalani sandstones show wide range with highly variable amount comparable with moderate to high chemical weathering (Fig. 13). The CIA values are in good agreement with those of PIA and CIW and show a good linear relationship (Fig. 13). The variations in CIA, PIA and CIW values may be due to the different concentrations of alumina in samples rather than variable degrees of source area weathering. Except for sample three, all the samples have CIA, PIA and CIW values more than 68 (Table 1). This reflects the moderate and high weathering conditions either in the original source terrane or during transportation before deposition. Moreover, high CIA values, suggest derivation from a stable cratonic source (Hossain *et al*., 2010).

Also, PIA values indicate that the plagioclases in the possible parent rock displayed high weathering condition and resulted in low CaO content, especially with increasing PIA values. This implies that with increasing chemical weathering the sediments are steadily depleted in plagioclases and enriched in secondary aluminous clay minerals (Roy *et al*., 2008).

Some elemental ratios, Al/Na, Al/K, Ti/Na, K/Na and Rb/K were used also as markers for intensities of chemical weathering (Roy *et al*., 2008). These ratios progressively increase with increasing chemical weathering. Such case may be referred to the solubility and ion potential where labile cations (Na, K, Ca, Rb) are leached in favorite to insoluble hydrolysates (Ti, Al) (Nesbitt and Young, 1982; Roy *et al*., 2008). However, it is indicated that both K and Rb are integrated into clay minerals by adsorption and cation exchange during initial weathering of fresh rocks. But, with increasing weathering, K is preferentially leached compared to Rb (Wronkiewicz and Condie, 1989). Following Roy *et al*. (2008), plots of the present CIA values against Al/Na, Al/K, Ti/Na, K/Na and Rb/K elemental ratios (molar proportion; Fig. 13) support the intermediate to extreme chemical weathering.

The CIA data are presented graphically on the Al_2O_3-(CaO^*+Na_2O)-K_2O (A-CN-K) ternary diagram (Nesbitt and Young, 1984). This can helps to understand the trends of chemical weathering, infer bulk source composition and the extent of post-depositional K-metasomatism, if present. Additionally, the role of steady-state or non-steady state weathering can be evaluated (Nesbitt and Young, 1984; Fedo *et al*., 1995; Roy *et al*., 2008; Hossain *et al*., 2010). In the A-CN-K diagram (Fig. 14), the studied sandstones commonly form a weathering trend that is almost parallel to the A-CN line. All the studied samples plot away from the plagioclase K-feldspar line in a direction towards the A apex (i.e., near to the highly weathered minerals). The increases in CIA

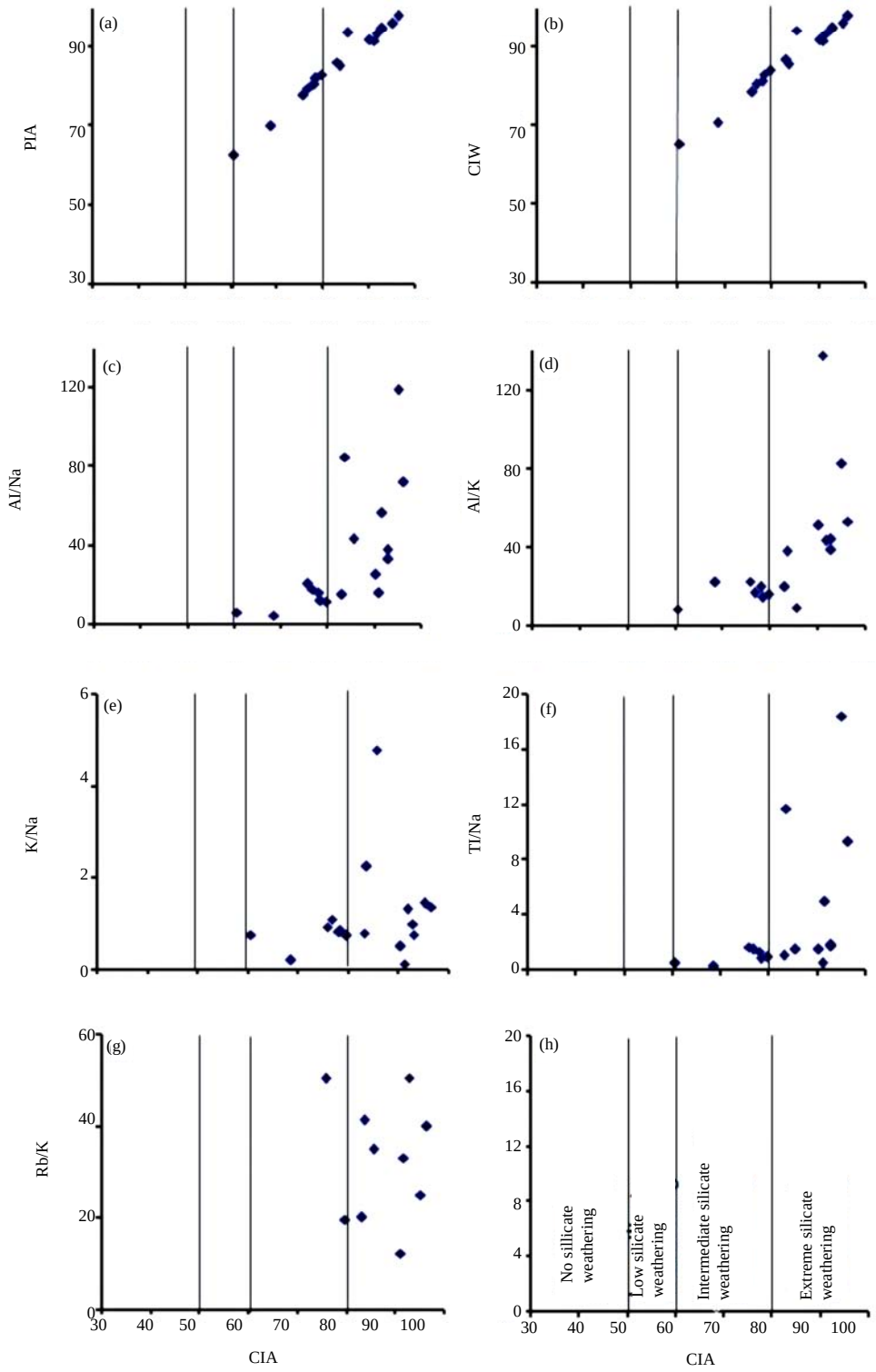

Fig. 13: Scatter plots of chemical index of alteration (CIA) vs. PIA, CIW, Al/Na, Al/K, K/Na, Ti/Na and Rb/K showing the degrees of chemical weathering in G. Ghazalani sediments

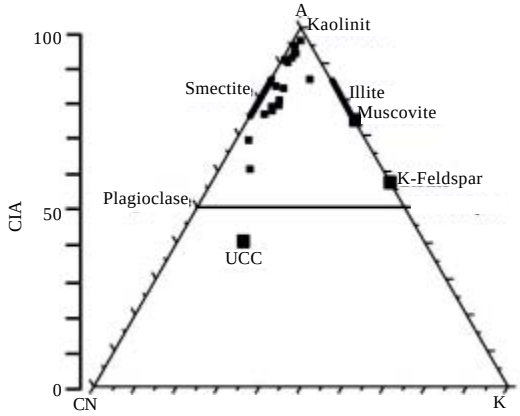

Fig. 14: The Al_2O_3-(CaO+Na_2O)-K_2O (A-CN-K) ternary diagram in molecular proportions for G. Ghazalani sandstones (after Nesbitt and Young, 1984). Also plotted is the average upper continental crust (Taylor and McLennan, (1985)), as well as some rock forming minerals important in silicate rock weathering

values possibly reflect increasing proportions of clay minerals with respect to feldspar. This will lead to increase proportion of Al_2O_3-rich clay minerals (e.g., kaolinite). In turn, it reflects that these samples experienced steady state weathering, supporting a stable and intensely weathered source interpretation (Nesbitt *et al*., 1997). This can be interpreted as progressive removal of labile cations as is commonly done for weathering profiles; also, indicates that more mature material is being supplied to the basin of deposition.

Low content of K_2O in G. Gazalani sandstones may be ascribed to intense chemical weathering (Cox *et al*., 1995) which enhanced leaching of soils and removal of alkalis in solution. Very low K_2O/Al_2O_3 ratios (0.01-0.11, average: 0.04), caused by the presence of high proportion of kaolinite, possibly indicate moderate to intense chemical weathering of source rocks (Potter *et al*., 1980). This is confirmed by the mineralogical analysis that revealed presence of kaolinite as sole clay mineral or kaolinite with minor illite. This compositionally mature sandstones possibly support deposition in a tectonically quiescent or cratonic setting where recycling and associated weathering were active during such sustained periods of tectonic quiescence (Taylor and McLennan, 1985). However, intense chemical weathering of first-cycle detritus can also produce sandstones as mature as those of the pre-Cenomanian sandstones (Barshad, 1966; Ghosh and Sarkar, 2010).

Lacks of epeirogenic movements during Early Cretaceous time corroborated such tectonic quiescence conditions and reflect that relief and rate of mechanical erosion were insignificant. Moreover, tectonic quiescence coincided in time with the warm and humid climate conditions that prevailed in the Egyptian territory during Paleozoic to pre-Cenomanian and mostly in Early Cretaceous times (Said *et al*., 1976). Such conditions let to increase the intensity of chemical weathering and the decomposition of the source area parent rocks.

High ratio of Th/U reflects intense weathering condition, ratio increases with kaolinite content, with the highest value in the more deeply weathered rocks (McLennan *et al*., 1990). However, the Th/U ratios can also change due to differences in oxidation state and therefore do not necessarily reflect source-area weathering conditions (Bauluz *et al*., 2000; Joo *et al*., 2005). The presence of correlation between Th/U ratios and CIA values (r = 0.41) suggests that the Th/U ratios are probably a reflection of chemical weathering rather than a result from changes in redox conditions during diagenesis.

Variation in REE contents in sediments may be related either to weathering or to variations in grain-size fractions and mineral contents due to hydraulic sorting (Cullers *et al*., 1975; McLennan, 1989). During weathering the REE are relatively immobile, so only minor enrichment or loss is expected. However, the LREE and HREE show different types of behavior and may become fractionated (Condie *et al*., 1995). Another possibility for the variations in ΣREE content among the studied sandstones can be related to an influence of a quartz dilution effect on abundance of heavy minerals and/or clay (Taylor and Mclennan, 1985; Armstrong-Altrin *et al*., 2004). Thus, we interpret the differences in ΣREE content of the pre-Cenomanian sandstones may be due to influence of a quartz dilution. This interpretation is supported by the significant good correlation between the LREEs, HREEs and ΣREE and Al_2O_3 (r = 72, 75 and 73, respectively). The average ΣREE contents in clay rich samples (contain higher Al_2O_3 concentration) is about 2.5 times higher than those contain less alumina; this strongly suggests that the REE are hosted mainly in the sample rich in clay content rather than those rich in quartz as reported by Taylor and McLennan (1985). On the other hand, clays are not the sole responsible for the variation in REE contents. Zircon ($ZrSiO_4$), as a heavy mineral, is enriched in HREE and Hf (Taylor and McLennan, 1985; Borges *et al*., 2008; Mahjoor *et al*., 2009). Presence of very good correlation between Zr and Hf (r = 1) and a good correlation between Zr and Yb as representative of

HREE (r = 0.88) suggest that zircon controls the values of HREE and Hf in the studied pre-Cenomanian sandstones.

Ce fractionation can take place at some stage in weathering and sedimentary processes. In the early stages, negative Ce-anomalies are noticed in weathering products like secondary hydrous phosphates (Braun *et al*., 1998) and positive Ce-anomalies emerge in deeply weathered and lateritic profiles where soluble Ce^{3+} oxidizes to insoluble, stable Ce^{4+} and hosted in secondary cerianite, $Ce(IV)O_2$(Braun *et al*., 1998; Borges *et al*., 2008). The relatively high positive Ce anomaly of G. Ghazalani sandstone samples (Ce/Ce* range from 1.03-1.25 average 1.07; Table 3) support that the source area had experienced intensive chemical weathering. This interpretation is consistent with the occurrence of kaolin deposits located at the base of many sandstone successions belong to the pre-Cenomanian (example, Early Cretaceous) in different localities in Sinai. This kaolin deposits were formed as a result of extensive chemical weathering (laterizing conditions) that led to the development of kaolinitic profiles on the parent source rocks, then, later on, were carried out to the basins of deposition (Yanni, 1987).

The recycling influence can also be recognized on the Th/Co vs. Zr/Co plot (Fig. 12b). Zr is the physically and chemically ultra-stable mineral zircon that can indicate the effect of recycling (McLennan *et al*., 1993; Borges *et al*., 2008). In that plot (Fig. 12b) most of studied samples demonstrate a linear compositional trend, with some spread toward recycling.

The mobile elements Na_2O, K_2O, MgO and P_2O_5 were depleted in respect to the UCC which is reliable with the loss through sedimentary processes. Depletion in Al_2O_3 and enrichment in SiO_2 relative to the UCC may be due to sedimentary sorting and loss of small grain-sized clays (Al_2O_3-rich and SiO_2-poor) and retention of sand-size composition (Al_2O_3-poor and SiO_2-rich) (Borges *et al*., 2008).

The SiO_2/Al_2O_3 is a commonly employed index of sedimentary maturation. Values increase because of increase of quartz at the expense of less resistant components such as feldspar and lithic fragments during sediment transport and recycling. The SiO_2/Al_2O_3 ratio is about 3 in basic rocks (basalts and Gabbros) and it is around 5 In the acidic end member (granites and rahyolites) (Le Maitre, 1976; Roser *et al*., 1996). Ratio more than 5 or 6 in sedimentary rocks provided evidence of sedimentary maturation (Roser *et al*., 1996). The average value of SiO_2/Al_2O_3 ratio for the studied sandstones is about 48 which is significantly high, indicating highly mature sediments. Moreover, if we omit the obvious higher values (samples 3, 8 and 12, Table 1), the SiO_2/Al_2O_3 = 33.80 which is strongly comparable to the value of 30 reported in the modern sediment (Valloni and Maynard, 1981; McLennan *et al*., 1990) that interpreted as highly mature sediments. The dominant of quartz arenites as well as presence of the ultra-stable clay minerals kaolinite and illite, identified within the clay fractions of these sandstones, is an additional criterion for their high maturity.

CONCLUSIONS

The pre-Cenomanian sandstone sequence (~ 214 m thick) exposed at Gebel Ghazalani area, East Sinai starts at the base by Lower Paleozoic pre-Carboniferous sandstones that unconformably overlies the Katherina Volcanics and followed unconformably upwards by the Lower Cretaceous sediments of the Malha Formation which underlies the Cenomanian shales and marls. Geochemically, the Pre-Cenomanian sandstones are mainly classified as quartz arenite with few sublitharenite and rare litharenite and wacke. Major, trace elements and REE ratios and diagrams suggest that sediments were deposited in a passive margin and the sediments were derived from felsic (granitic) source rocks. The source area may have contained quartzose sedimentary rocks. The G. Ghazalani sediments deposited in the passive margin setting resemble to those of the Atlantic type sediments and can be categorized by higher Zr contents, higher Zr/Nb, Zr/Th ratios and lower Rb, V and Ti/Zr ratio. These features mirror the recycling of these sediments, the depletion of feldspar and labile fragments and the increased abundance of heavy minerals, mainly zircon, through sedimentary processes. The values of the weathering indices (CIA, PIA and CIW) along with the elemental molar ratios suggest moderate to extreme weathering conditions in the source area and/or during transportation. Most of the studied sandstones are inferred as highly mature sediments evidenced from their high SiO_2/Al_2O_3 ratio (47.94) and the presence of the ultra-stable clay minerals, Kaolinite and illite. Chondrite-normalized REE patterns for most of the sandstone samples display high LREE/HREE ratio, flat HREE pattern and pronounced negative Eu anomaly and in general correlate well with the UCC and PAAS average composition.

REFERENCES

Abd El-Khalek, M.L.A., N.A. Abd El-Wahed and A.A. Sehim, 1993. Wrenching deformation and tectonic setting of the northwestern part of the Gulf of Aqaba. Geol. Soc. Egypt Spec. Pub., 1: 409-444.

Abd El-Rahman, Y., A. Polat, B.J. Fryer, Y. Dilek, M. El-Sharkawy and S. Sakran, 2010. The provenance and tectonic setting of the Neoproterozoic Um Hassa Greywacke Member, Wadi Hammamat area, Egypt: Evidence from petrography and geochemistry. J. Afri. Earth Sci., 58: 185-196.

Abdallah, A.M. and A. El-Adindani, 1963. Stratigraphy of the upper paleozoic rocks, western side of Gulf of Suez. Egypt. Geol. Surv. Egypt, 25: 18-18.

Abu-Zeid, M.M., K.M. Amer, N.N. Yanni and S.S. El-Wekeil, 1991. Petrology, mineralogy and sedimentation of the Paleozoic sequence of Gabal Qattar, Wadi Feiran, Sinai. Egypt. J. Geol., 34: 145-169.

Ajayi, T.R., A.A. Oyawale, F.Y. Islander, O.I. Asubiojo, D.E. Klein and A.I. Adediran, 2006. Trace and rare earth elements geochemistry of oshosun sediments of dahomey basin, Southwestern Nigeria. J. Applied Sci., 6: 2067-2076.

Akarish, A.I.M., 1998. Paleozoic-Paleocene stratigraphy of the Taba-Nuweiba area. East Sinai M.E.R.C. Ain Shams Univ. Earth Sci. Ser., 12: 48-64.

Akarish, A.I.M. and A.M. El-Gohary, 2008. Petrography and geochemistry of lower Paleozoic sandstones, East Sinai, Egypt: Implications for provenance and tectonic setting. J. Afri. Earth Sci., 52: 43-54.

Armstrong-Altrin, J.S., Y.L. Lee, S.P. Verma and S. Ramasamy, 2004. Geochemistry of sandstones from the upper Miocene Kudankulam formation, Suthern India: Implications for provenance, weathering and tectonic setting. J. Sediment. Res., 74: 285-297.

Asiedu, D.K., E. Hegner, A. Rocholl and D. Atta-Peters, 2005. Provenance of late Ordovician to early Cretaceous sedimentary rocks from southern Ghana, as inferred from Nd isotopes and trace elements. J. Afri. Earth Sci., 41: 316-328.

Barshad, I., 1966. The effect of a variation in precipitation on the nature of clay mineral formation in soils from acid and basic igneous rocks. Proc. Int. Clay Conf. Jerusalem, Israel, 1: 167-173.

Bauluz, B., M.J. Mayayo, C. Fernandez-Nieto and J.M.G. Lopez, 2000. Geochemistry of Precambrian and Paleozoic siliciclastic rocks from the Iberian Range (NE Spain): implication for source-area weathering, sorting, provenance and tectonic setting. Chem. Geol., 168: 135-150.

Bhatia, M.R., 1983. Plate tectonics and geochemical composition of sandstones. J. Geol., 91: 611-627.

Bhatia, M.R. and K.A.W. Crook, 1986. Trace element characteristics of graywackes and tectonic setting discrimination of sedimentary basins. Contrib. Mineral. Petrol., 92: 181-193.

Borges, J.B., Y. Huh, S. Moon and H. Noh, 2008. Provenance and weathering control on river bed sediments of the eastern Tibetan Plateau and the Russian Far East. Chem. Geol., 254: 52-72.

Braun, J.J., J. Viers, B. Dupre, M. Polve, J. Ndam and J.P. Muller, 1998. Solid/liquid REE fractionation in the lateritic system of Goyoum, East Cameroon: The implication for the present dynamics of the soil covers of the humid tropical regions. Geochim. Cosmochim. Acta, 62: 273-299.

Brindley, G.W., 1961. Kaolin, Serpentine and Kindred Minerals. In: The X-ray Identification and Crystal Structure of Clay Minerals, Brown, G. (Ed.). 2nd Edn., Mineralogical Society, London, pp: 51-131.

Condie, K.C., J. Dengate and R.L. Cullers, 1995. Behavior of rare earth elements in a paleoweathering profile on granodiorite in the front range, Colorado, USA. Geochim. Cosmochim. Acta, 5: 279-294.

Cox, R., D.R. Lowe and R.L. Cullers, 1995. The influence of sediment recycling and basement composition on evolution of mudrock chemistry in the south-western United States. Geochim. Cosmochim. Acta, 59: 2919-2940.

Crook, K.A.W., 1974. Lithostratigraphy and Geotectonic: The Significance of Composition Variation in *Flysch arenites* (graywakes). In: Modern and Ancient Geosynclinal Sedimentation, Dott, R.H. and R.H. Shaver (Eds.). Society of Economic Paleontologists and Mineralogists, Tulsa, Okla., USA., pp: 304-310.

Cullers, R.L. and J.L. Graf, 1984. Rare-earth elements in Igneous Rocks of the Continental Crust: Intermediate and Silicic Rocks-Ore Petrogenesis. In: Rare Earth Element Geochemistry, Henderson, P. (Ed.). Elsevier, Amsterdam, pp: 275-316.

Cullers, R.L., A. Basu and L.J. Suttner, 1988. Geochemical signature of provenance in sand-size material in soils and stream sediments near the Tobacco Root batholith, Montana, USA. Chem. Geol., 70: 335-348.

Cullers, R.L., 1994. The controls on the major-and trace-element variation of shales, siltstones and sandstones of Pennsylvanian-Permian age from uplifted continental blocks in Colorado to platform sediments in Kansas, USA. Geochim. Cosmochim. Acta, 58: 4955-4972.

Cullers, R.L., 2000. The geochemistry of shales, siltstones and sandstones of Pennsylvanian-Permian age, Colorado, USA: Implications for provenance and metamorphic studies. Lithos, 51: 181-203.

Cullers, R.L. and V.N. Podkovyrov, 2000. Geochemistry of the Mesoproterozoic Lakhanda shales in southeastern Yakutia, Russia: Implications for mineralogical and provenance control and recycling. Precamb. Res., 104: 77-93.

Cullers, R.L., S. Chaudhuri, B. Arnold, M. Lee and C.W. Jr. Wolf, 1975. Rare-earth distributions in clay minerals and clay-sized fractions of lower permian Havensville and Eskridge shales of Kansas and Oklahoma. Geochim. Cosmochim. Acta, 39: 1691-1703.

El-Kelany, A. and M. Said, 1990. Lithostratigraphy of southeastern Sinai. Ann. Geol. Surv. Egypt, 16: 215-221.

Fedo, C.M., H.W. Nesbitt and G.M. Young, 1995. Unraveling the effects of potassium metasomatism in sedimentary rocks and paleosols, with implications for paleoweathering conditions and provenance. Geology, 23: 921-924.

Fedo, C.M., K.A. Eriksson and E.J. Krogstad, 1996. Geochemistry of shales from the Archean (3.0 Ga.) Buhwa Greenstone Belt. Zimbabwe: Implications for provenance and source area weathering. Geochim. Cosmochim. Acta, 60: 1751-1763.

Feng, R. and R. Kerrich, 1990. Geochemistry of fine grained clastic sediments in the Archean Abitibi greenstones belt, Canada: Implications for provenance and tectonic setting. Geochim. Cosmochim. Acta, 54: 1061-1081.

Gallala, W.E., M.E. Gaied and M. Montacer, 2009. Detrital mode, mineralogy and geochemistry of the Sidi Aich Formation (*Early Cretaceous*) in central and southwestern Tunisia: Implications for provenance, tectonic setting and paleoenvironment. J. Afri.Earth Sci., 53: 159-170.

Garver, J.I., P.R. Royce and T.A. Smick, 1996. Chromium and nickel in shale of the Taconic Foreland: A case study for the provenance of fine-grained sediments with an ultramafic source. J. Sediment. Res., 66: 100-106.

Ghosh, S. and S. Sarkar, 2010. Geochemistry of Permo-Triassic mudstone of the Satpura Gondwana basin, central India: Clues for provenance. Chem. Geol., 277: 78-100.

Herron, M.M., 1988. Geochemical classification of terrigenous sands and shales from core or log data. J. Sediment Petrol., 58: 820-829.

Hirst, D.M., 1962. The geochemistry of modern sediments from the Gulf of Paria. II. The location and distribution of trace elements. Geochim. Cosmochim. Acta, 26: 1174-1187.

Hossain, H.M.Z., B.P. Roser and J.I. Kimura, 2010. Petrography and whole-rock geochemistry of the Tertiary Sylhet succession, northeastern Bengal Basin, Bangladesh: Provenance and source area weathering. Sediment. Geol., 228: 171-183.

Issawi, B., M. El-Hinnawi, M. Francis and A. Mazhar, 1999. The phanerozoic geology of Egypt: A geodynamic approach. Special Publication No. 76, The Egyptian Geological Survey, Egypt, pp: 472.

Jin, Z., F. Li, J. Cao, S. Wang and J. Yu, 2006. Geochemistry of Daihai Lake sediments, Inner Mongolia, north China: Implications for provenance, sedimentary sorting and catchment weathering. Geomorphol., 80: 147-163.

Joo, Y.J., Y. Lee and Z. Baib, 2005. Provenance of the Qingshuijian Formation (*Late Carboniferous*), NE China: Implications for tectonic processes in the northern margin of the North China block. Sediment. Geol., 177: 97-114.

Keller, W.D., 1956. Clay minerals as influenced by environments of their formation. Bull. Am. Assoc. Pet. Geol., 40: 2689-2710.

Klitzsch, E., F.K. List and G. Pohlmann, 1986. Geological map of Egypt (1:500 000 in 20 sheets). Conoco Coral and Egyptian General Petroleum Corporation, Cairo.

Kora, M., 1991. Lithostratigraphy of the Early Paleozoic succession in Ras El-Naqb area, east central Sinai, Egypt. Newsl. Stratig., 24: 45-57.

Kostandi, A.B., 1959. Facies maps for the study of Paleozoic and Mesozoic Sedimentary basins of the Egyptian Region. 1st Arab Petrol. Congr. Cairo, 2: 54-62.

Le Maitre, R.W., 1976. The chemical variability of some common igneous rocks. J. Petrol., 17: 589-637.

Lee, Y.I.I., 2002. Provenance derived from the geochemistry of late Paleozoic-early Mesozoic mudrocks of the Pyeongan Supergroup, Korea. Sediment. Geol., 149: 219-235.

Lonnie, T.P., 1982. Mineralogic and chemical composition of marine and nonmarine transitional clay beds on south shore of Long Island, New York. J. Sediment. Petrol., 52: 529-536.

Mader, D. and F. Neubauer, 2004. Provenance of Palaeozoic sandstones from the Carnic Alps (Austria): Petrographic and geochemical indicators. Int. J. Earth Sci., 93: 262-281.

Mahjoor, A.S., M. Karimi and A. Rastegarlari, 2009. Mineralogical and geochemical characteristics of clay deposits from South Abarkouh district of Clay Deposit (Central Iran) and their applications. J. Applied Sci., 9: 601-614.

McLennan, S.M., W.B. Nance and S.R. Taylor, 1980. Rare earth element-thorium correlations in sedimentary rocks and the composition of the continental crust. Geochim. Cosmochim. Acta, 44: 1833-1839.

McLennan, S.M., 1989. Rare earth elements in sedimentary rocks: Influence of provenance and sedimentary processes. Geochemistry and mineralogy of the rare earth elements. Rev. Mineral. Geochem., 21: 169-200.

McLennan, S.M., S.R. Taylor, M.T. Mcculloch and J.B. Maynard, 1990. Geochemical and Nd-Sr isotopic composition of deep-sea turbidites: Crustal evolution and plate tectonic associations. Geochim. Cosmochim Acta, 54: 2015-2050.

McLennan, S.M., S. Hemming, D.K. McDaniel and G.N. Hanson, 1993. Geochemical Approaches to Sedimentation, Provenance and Tectonics. In: Processes Controlling the Composition of Clastic Sediments, Johnson, M.J. and A. Basu (Eds.). Geological Society of Amercan Special Paper, USA., pp: 21-40.

Nagarajani, R., J.S. Armstrong-Altrin, R. Nagendra, J. Madhavaraju and J. Moutte, 2007. Petrography and Geochemistry of Terrigenous Sedimentary Rocks in the Neoproterozoic Rabanpalli Formation, Bhima Basin, Southern India: Implications for Paleoweathering Conditions, Provenance and Source Rock Composition. J. Geol. Soc. India, 70: 297-312.

Nesbitt, H.W. and G.M. Young, 1982. Early proterozoic climates and plate motions inferred from major element chemistry of lutites. Nature, 299: 715-717.

Nesbitt, H.W. and G.M. Young, 1984. Prediction of some weathering trends of plutonic and volcanic rocks based on thermodynamic and kinetic considerations. Geochim. Cosmochim. Acta, 48: 1523-1534.

Nesbitt, H.W., C.M. Fedo and G.M. Young, 1997. Quartz and feldspar stability, steady and non-steady-state weathering and petrogenesis of siliciclastic sands and muds. J. Geol., 105: 173-191.

Potter, P.E., J.B. Maynard and W.A. Pryor, 1980. Sedimentology of Shale: Study Guide and Reference Source. 2nd Edn., Springer-Verlag, Berlin, ISBN,13: 9780387904306. pp: 306.

Roser, B.P. and R.J. Korsch, 1986. Determination of tectonic setting of sandstone-mudstone suites using SiO2 content and K2O/Na2O ratio. J. Geol., 94: 635-650.

Roser, B.P. and R.J. Korsch, 1988. Provenance signature of sandstone-mudstone suite determined using discriminant function analysis of major element data. Chem. Geol., 67: 119-139.

Roser, B.P., R.A. Cooper, S. Nathan and A.J. Tulloch, 1996. Reconnaissance sandstone geochemistry, provenance and tectonic setting of the lower Paleozoic terraines of the West Coast and Nelson, New Zealand. New Zealand J. Geol. Geophys, 39: 1-16.

Roy, P.D., M. Caballeroa, R. Lozanoc and W. Smykatz-Klossd, 2008. Geochemistry of late quaternary sediments from Tecocomulco lake, central Mexico: Implication to chemical weathering and provenance. Chemie der Erde, 68: 383-393.

Said, R., 1962. The Geology of Egypt. Elsevier Publication, Amsterdam.

Said, R., 1971. Explanatory Notes to Accompany the Geological Map of Egypt. Ministry of Industry, Egypt, pp: 123.

Said, R., A.H. Sabet, A.A. Zalata, V.A. Toniakov and V.I. Pokryshin, 1976. A review of theories on the geological distribution of bauxite and their application for bauxite prospecting in Egypt. Ann. Geol. Surv. Egypt, 6: 6-32.

Salem, A.M., A.T. Abd El-hamed, I. Hassanein and A.M. Fouda, 2001. Diagenetic implications and provenance of pre-Cenomanian sandstones, Sheikh Attia Area, East- Central Sinai, Egypt. Sediment. Egypt, 9: 57-72.

Samuel, M.D., H.E. Moussa and M.K. Azer, 2007. A-type volcanics in Central Eastern Sinai, Egypt. J. Afri. Earth Sci., 52: 203-226.

Taylor, S.R. and S.M. McLennan, 1985. The Continental Crust: Its Composition and Evolution. Blackwell, Oxford, ISBN-13: 978-0632011483, pp: 312.

Tucker, M.E., 1988. Techniques in Sedimentology. Blackwell Sci. Publ, Oxford, ISBN-10: 0632013613, pp: 391.

Turekian, K.K. and H.C. Michael, 1960. The geochemistries of chromium, cobalt and nickel. Inter. Geol. Cong., 1: 14-27.

Valloni, R. and J.B. Maynard, 1981. Detrital moded of recent deep sea sands and their relation to tectonic setting: A first approximation. Sedimentol., 28: 75-83.

Wronkiewicz, D.J. and K.C. Condie, 1989. Geochemistry and provenance of sediments from the pongola supergroup, South Africa: Evidence for a 3.0 Ga old continental craton. Geochim. Cosmochim. Acta, 53: 1537-1549.

Yanni, N.N., 1987. Characteristics of lower cretaceous kaolin deposits, West Central Sinai. Egypt J. Geol., 31: 129-141.